LANGMUIR Article
Cite This: Langmuir 2018, 34, 12934−12946
pubs.acs.org/Langmuir

Attainment of Water and Oil Repellency for Engineering Thermoplastics without Long-Chain Perfluoroalkyls: Perfluoropolyether-Based Triblock Polyester Additives

Liying Wei,[†] Tugba Demir,[†,‡] Anise Grant,[§] Vladimir Tsukruk,[§] Philip J. Brown,[†] and Igor Luzinov*[,†]

[†]Department of Materials Science and Engineering, Clemson University, Clemson, South Carolina 29634, United States
[‡]Department of Chemical Engineering, Faculty of Engineering, Ankara University, Tandogan, 06100 Ankara, Turkey
[§]School of Materials Science and Engineering, Georgia Institute of Technology, Atlanta, Georgia 30332, United States

Supporting Information

ABSTRACT: For decades, water and oil repellency of engineering thermoplastics has been achieved with introduction of long-chain perfluoroalkyl substances and moieties (C_nF_{2n+1}, $n \geq 7$). However, their bioaccumulative and toxicological impact is now widely recognized and, consequently, the substances have been phased out of industrial production and applications. To this end, we have synthesized fluorinated oligomeric triblock polyesters (FOPBs), which do not possess the long-chain perfluoroalkyl segments and serve as effective low-surface-energy additives to engineering thermoplastics. More specifically, we obtained original perfluoropolyether (PFPE)-based triblock copolymers, in which two identical fluorinated blocks were separated by a short nonfluorinated polyester block made of poly(ethylene isophthalate) (PEI). It was found that when FOPBs were added to poly(ethylene terephthalate), nylon-6, and poly(methyl methacrylate) films they readily migrate to the film surface and in doing so imparted significant water and oil repellency to the thermoplastic boundary. The water/oil wettability of the films modified with FOPB is considerably lower than the wettability of the films modified with an analogous PFPE-based polyester, which differs from FOPB only by the absence of the short nonfluorinated PEI middle block. We associate the superiority of the triblock copolymers in terms of water and oil repellency with their ability to form brushlike structures on polymer film surfaces.

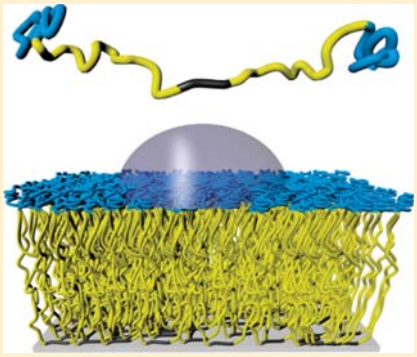

INTRODUCTION

For decades, water and oil repellency has been one of the major targets in the design of practical polymer-based materials. Until recently, long-chain perfluoroalkyl substances and moieties (PFASs, C_nF_{2n+1}, $n \geq 7$) have been practically exclusively used for this purpose in numerous applications, including textiles, polymer films, and surfactants.[1−4] However, their bioaccumulative and toxicological impact on environment, humans, and wildlife is now widely recognized and, consequently, the PFASs have been phased out of industrial production and applications.[1,5−7] On the other hand, PFASs with fewer than seven carbons are generally less toxic and less bioaccumulative in wildlife and humans.[8] To this end, our work reported here focuses on the enhancement of the water and oil repellency properties of engineering thermoplastics via addition of perfluoropolyether (PFPE)-based polyester triblock copolymers containing C_4F_9- and $C_6F_{13}-$ end groups. PFPEs (having in their backbone $-CF_2-$, $-CF_2-CF_2-$, and $-CF(CF_3)-CF_2-$ units that are separated by oxygen atoms) are considered as potentially safer substitutes for PFASs.[1,9,10] Indeed, PFPEs possess low surface tension (20−22 mN/m), low volatility, high chemical inertness and radiation resistance, optical transparency, nonflamability, good oxidative/thermal stability, low coefficient of friction, and low toxicity.[11−16] Although PFPEs have numerous advantages, as pure materials, they cannot serve as effective water/oil repellent additives for conventional thermoplastics due to their immiscibility and incompatibility with polymer matrices.[11,17] In addition, the materials are liquids of very low viscosity, which leads to an exudation from the surface of the host polymer over short periods of time.

In this respect, PFPE-based cross-linked materials and copolymers have been demonstrated to have the capability to function as hydrophobic/lyophobic materials and interfaces.[9,11,13−21] These copolymers are also shown to be quite effective as additives that offer long-lasting surface modifications to polymer materials.[21,22] In the latter case, the compatibility between different segments can be controlled by the chemical composition and structure of nonfluorinated parts. For instance, Wang et al. described the modification of poly(butylene terephthalate) with fluorinated multiblock polyester containing PFPE segmens.[22] Drysdale et al. reported on the blending of poly(trimethylene terephthalate) with

Received: August 2, 2018
Revised: September 29, 2018
Published: October 1, 2018

DOI: 10.1021/acs.langmuir.8b02628
Langmuir 2018, 34, 12934−12946

blocky polyesters containing isophthalic units fluorinated with PFPE.[21]

In our recent study, it was demonstrated that PFPE-based oligomeric polyesters (FOPs) can also be employed as effective low-surface-energy additives to engineering thermoplastics.[10] In particular, we have synthesized FOPs with and without fluorinated end groups and blended them with poly(ethylene terephthalate) (PET). The polyesters terminated with fluorinated end groups contained only short C_4F_9- perfluoroalkyl segments, which cannot yield unsafe long-chain perfluoroalkyl carboxylic acids. To improve the compatibility of the materials with PET (and other polar thermoplastics), we introduced isophthalate (IPH) segments into the polyesters and targeted the synthesis of lower-molecular-weight oligomeric macromolecules. In addition, macromolecules of relatively low molecular weights (MWs) have relatively high rates of diffusion and, therefore, migrate readily to the material boundary. In fact, we found that when FOPs were added to PET films, they occupied the film surfaces and brought significant water and oil repellency to the thermoplastic boundary. We have established that the wettability of FOP/PET films depends on three main parameters: (i) end groups of fluorinated polyesters, (ii) concentration of fluorinated polyesters in films, and (iii) equilibration via annealing. The FOP most effective in water/oil repellency has two C_4F_9-PFPE$-$ tails (Figure 1a,c). The addition of this oligomeric polyester to PET materials allowed us to attain levels of oil repellency and surface energy comparable to those of poly(tetrafluoroethylene) (PTFE/Teflon), a fully perfluorinated polymer.

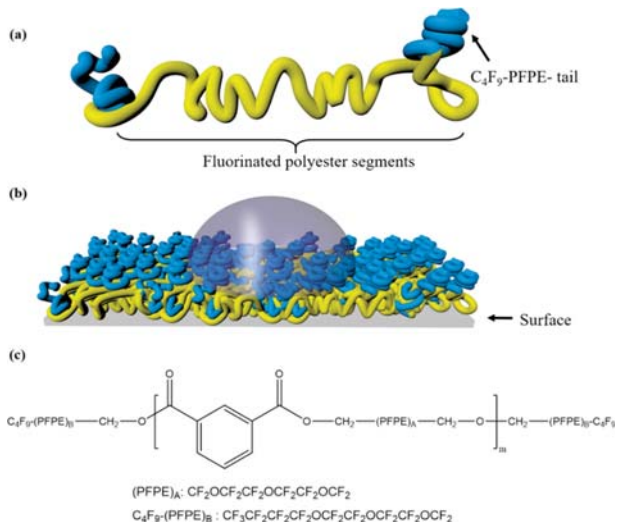

Figure 1. Schematic of FOP with two C_4F_9-PFPE$-$ tails (a); schematic of FOP chains spreading over the thermoplastic surface and contacting wetting liquid (b); and chemical structure of FOP with two C_4F_9-PFPE$-$ tails (c).

However, we also found that for the FOP/PET blend to demonstrate surface energies close to those of PTFE quite a significant concentration (~10−15%) of the fluorinated polyester has to be used. We have associated this phenomenon with the conformation of the FOP macromolecule on the film surface (Figure 1b). As determined in earlier studies of fluorinated materials,[23−26] their surface is always preferentially occupied by the fragments of the polymer chain with the lowest surface energy. For FOPs, the order in terms of surface energy is as follows: CF_3- < $-(CF_2)_3-$ < $-CF_2-CF_2-O-$ < nonfluorinated isophthalate (IPH) units. To reach the lowest surface energy, the surface has to be populated with C_4F_9-functional groups that possess lower surface energy than that of $-CF_2-CF_2-O-$ and IPH chain segments. We suggest that FOP chains are spreading over the surface at relatively low concentrations and that $-CF_2-CF_2-O-$ and even IPH chain segments can interact with a contacting liquid attempting to wet the boundary (Figure 1b). Therefore, a relatively high concentration of the fluorinated polyester is necessary to maximize the presence of C_4F_9- groups at the surface.

To this end, we now report on the synthesis and properties of the next generation of highly effective FOP-based low-surface-energy additives. Specifically, we synthesized two different PFPE-based polyester triblock copolymers (fluorinated oligomeric triblock polyesters (FOPBs)), where two longer FOP end blocks are separated by a short nonfluorinated polyester block made of poly(ethylene isophthalate), PEI (Figure 2). One of the copolymers was terminated with $C_6F_{13}-$ end segments (**FOPB-2**), which are widely used since C_6-based materials have been considered as the most effective alternatives to PFASs having $C_7F_{15}-$ or longer perfluorinated moieties. The other copolymer possessed C_4F_9-PFPE$-$ end groups (**FOPB-1**), which had a shorter perfluorinated moiety and also contained oxygen atoms. In our study, we have compared the efficiency of these FOPBs as water/oil repellent additives to that of thermoplastic materials. We foresaw that the FOPB structure will support the formation of FOP brushlike layers on the surface, in which short perfluoroalkyl groups concentrate on the exterior of the thermoplastic film (Figure 2b). Formation of the brush is supported by segregation of the middle nonfluorinated block to the higher-surface-energy thermoplastic surface. The segregation is driven by the thermodynamic conditions of minimization of interfacial energy. In fact, PET, nylon-6, and poly(methyl methacrylate) (PMMA) films modified with just 5% of FOPB materials demonstrated wettability and surface energies close to or lower than those of PTFE. We also found that copolymers possessing $C_6F_{13}-$ and C_4F_9-PFPE$-$ end groups demonstrated comparable level of water and oil repellency.

EXPERIMENTAL SECTION

Materials. A telechelic PEI oligomer was synthesized by the solution reaction of isophthaloyl chloride (IsoCl) with ethylene glycol (EG), which were both purchased from Sigma-Aldrich. Semitelechelic PFPE-based polyester oligomers were synthesized through the reaction of IsoCl with fluorinated ether alcohols, such as 1*H*,1*H*-perfluoro-1-heptanol ($C_6F_{13}-$OH) from Matrix Scientific, 1*H*,1*H*-perfluoro-3,6,9-tiroxatridecan-1-ol (C_4F_9-PFPE$-$OH), and 1*H*,1*H*,11*H*,11*H*- perfluoro-3,6,9-trioxaundecane-1,11-diol (PFPE-diol) from Synquest Laboratories. In the synthesis of PEI and FOP oligomers, methyl ethyl ketone (MEK) from Alfa Aesar was dried by molecular sieves under vacuum and was used as a solvent. Triethylamine (Et_3N) used for the removal of HCl salt during synthesis was from Sigma-Aldrich. FOPBs were synthesized through melt polymerization of PEI with FOPs having different end groups. The solvent used for the polymer film fabrication, 1,1,1,3,3,3-hexafluoro-2-propanol (HFIP) from Oakwood Products, Inc., was used as received. Commercial-grade PET and nylon-6 pellets from Unifi and PMMA pellets from Sigma-Aldrich were used as received.

Synthesis of Poly(ethylene isophthalate) Oligomer. In the synthesis of the PEI oligomer, IsoCl was dissolved in MEK and preheated at 70 °C for 30 min. Then, EG and Et_3N in dry MEK were added to the IsoCl solution dropwise under vigorous stirring, and the

DOI: 10.1021/acs.langmuir.8b02628
Langmuir 2018, 34, 12934−12946

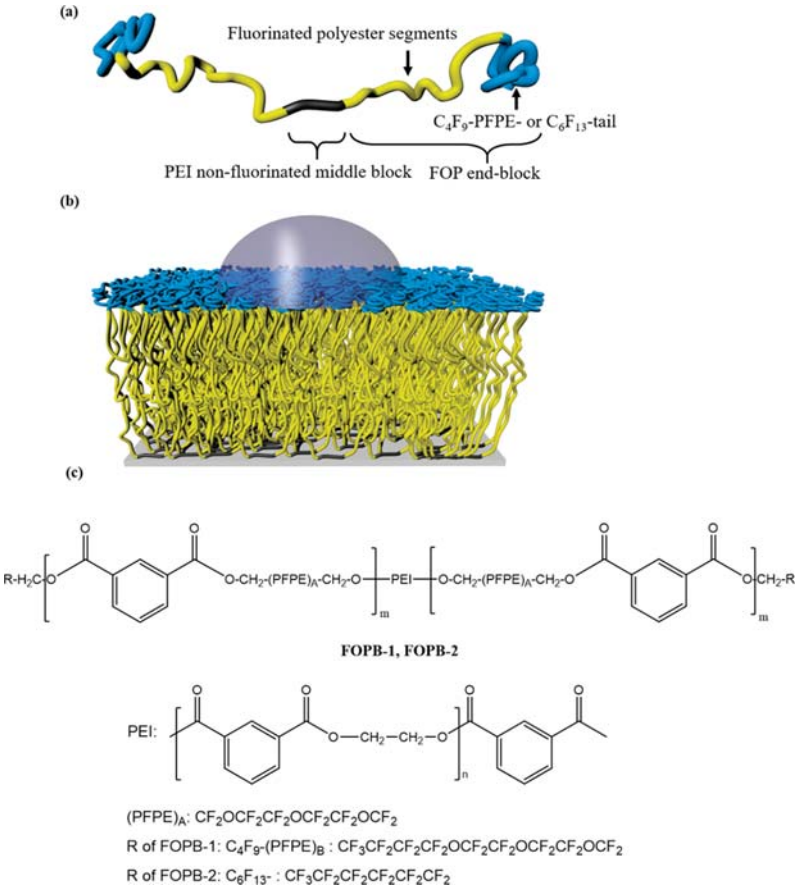

Figure 2. Schematic of FOPB with two perfluoroalkyl end segments (a); schematic of FOPB chains on the surface and contacting wetting liquid (b); and chemical structure of FOPBs (c).

solution was incubated at 70 °C for 3 h. After the formation of oligomers, the reaction mass was cooled down to room temperature and stirred overnight. Next, HCl salt trapped by Et_3N was removed by centrifugation at 5000 rpm for 1 h. The remaining solution was transferred to a 100 mL three-necked flask, which was equipped with a mechanical stirrer. The oligomer was heated at 50 °C for 4 h and at 70 °C for 1 h under a stream of nitrogen (N_2) to remove MEK. After MEK was removed, the reaction medium was heated at 100, 120, and 150 °C for 4, 2, and 7 h, respectively, under N_2 to obtain higher-molecular-weight macromolecules. The additional experimental details of the PEI synthesis are provided in the Supporting Information (SI) (Section S1).

Synthesis of Fluorinated Polyester Oligomers. For FOP synthesis, fluorinated ether alcohols and Et_3N were dissolved in dry MEK and preheated at 70 °C for 30 min with stirring. Then, the solution of IsoCl was added dropwise into the reaction media and the reaction was carried out at 70 °C for 3 h. Afterward, the solution was cooled down to room temperature and stirred overnight. After the reaction was completed, the Et_3N−HCl salt was removed at 5000 rpm for 1 h by centrifugation. The remaining solution was added to a 100 mL three-necked flask, equipped with a mechanical stirrer. The oligomers were heated at 50 and 70 °C for 4 and 1 h, respectively, under a stream of N_2 to remove MEK. After removal of MEK, the reaction medium was heated at 150 °C for 7 h under N_2 to obtain the targeted oligomers. The additional experimental details for the FOP synthesis are presented in SI (Section 1).

Synthesis of Fluorinated Block Copolymers. A telechelic PEI oligomer with reactive end groups was reacted with FOP semitelechelic oligomers in the melt state in a 100 mL three-necked flask to obtain fluorinated triblock copolymers. The reaction was carried out under N_2 at 200 °C for 5 h with vigorous stirring. The additional experimental details for FOPB synthesis are provided in the SI (Section 1).

Polymer Film Preparation. To prepare films, PET, PMMA, or nylon-6 was solvent-blended with FOPBs in HFIP at different concentrations. Polymer-blended films were fabricated on a clean Si wafer substrate by dip coating (dip coater: Mayer Fientechnik D-3400) from 3 wt % polymer solution in HFIP using 320 mm/min withdrawal rate. Prior to film deposition, the wafers were first cleaned in an ultrasonic bath for 30 min, placed in a hot "piranha" solution (3:1 concentrated sulfuric acid/30% hydrogen peroxide) for 1 h, and then rinsed several times with high-purity deionized water. After being rinsed, the substrates were dried under a stream of dry nitrogen. Afterward, the films were kept at room temperature overnight to allow for solvent evaporation. For selected experiments, the dried films were annealed at 140 °C for 3 h in a vacuum oven. The thickness of the polymer films was 300−350 nm as measured by ellipsometry.

Characterization Techniques. The molecular weight (MW) of the materials synthesized in this work was measured by gel permeation chromatography (GPC, Waters Breeze). Prior to the measurements, the oligomers were dissolved in chloroform and kept overnight. The obtained oligomer solutions were filtered through 0.2 μm syringe PTFE filters. Polystyrene was employed as a standard for the GPC calibration. Attenuated total reflectance Fourier transform infrared (ATR-FTIR) spectroscopy spectra of the materials were acquired with a Thermo Nicolet 6700 FTIR spectrometer. For fluorine nuclear magnetic resonance (^{19}F NMR) spectroscopy, the dried materials were dissolved in deuterated chloroform (with trichlorofluoromethane as a reference) for 24 h. A Bruker Avance II spectrometer (300 MHz) was used to record the ^{19}F NMR for the samples. For thermogravimetric analysis (TGA), PerkinElmer TGA was used. Samples of approximately 5 mg were pretreated under a

DOI: 10.1021/acs.langmuir.8b02628
Langmuir 2018, 34, 12934−12946

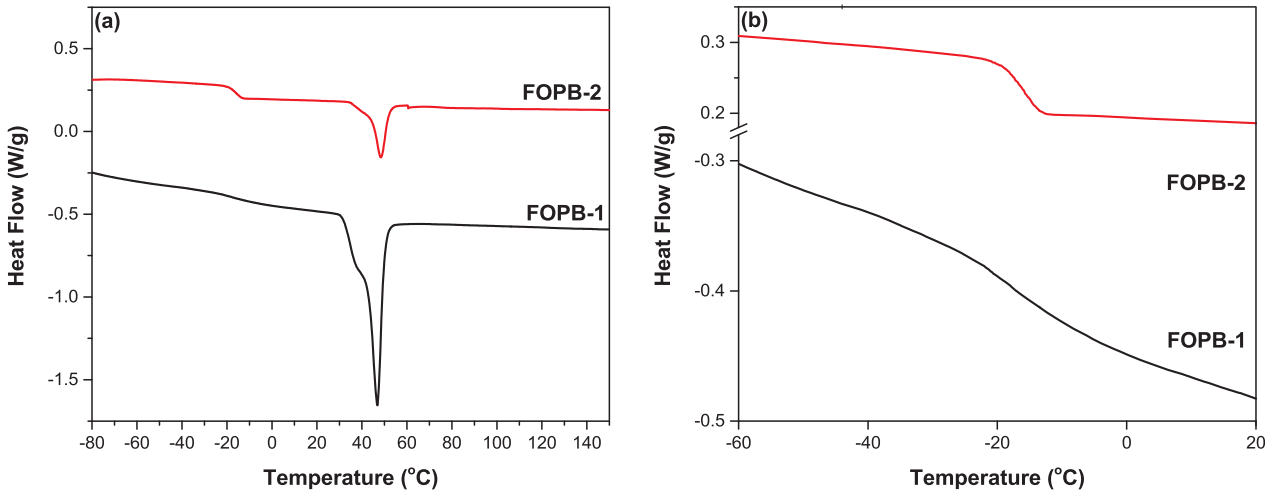

Figure 3. DSC traces for FOPBs (a) and for the T_g region of FOPBs (b).

nitrogen atmosphere (gas flow of 20 mL/min) for 10 min at 25 °C. Samples were heated to 600 °C at a heating rate of 20 °C/min under N_2. For differential scanning calorimetry (DSC), a DSC 2920 (TA Instruments) was employed. Samples (~5 mg) were analyzed at a heating rate of 20 °C/min under a nitrogen atmosphere. Atomic force microscopy (AFM, DI 3100 Dimensions) was conducted with a Dimension 3100 microscope (Digital Instruments, Inc.) to scan polymer films in tapping mode at 1 Hz scan rate. The static contact angles (CAs) of water and hexadecane (HCA) were measured at room temperature with an equilibration time of 30 s. CAs were recorded with a drop shape analysis instrument (DSA10, Kruss, Germany). X-ray photoelectron spectroscopy (XPS) spectra were obtained using a Thermo K-Alpha XPS (Thermo Fisher Scientific, West Palm Beach, FL) with monochromatic X-rays (Al Kα at 15 kV). The thickness of the films was determined by ellipsometry with a COMPEL automatic ellipsometer (InOm Tech, Inc.) at an angle of 70° and wavelength of 653 nm.

RESULTS AND DISCUSSION

PEI Middle Block. The telechelic poly(ethylene isophthalate) oligomer was synthesized to serve as a middle block in the triblock copolymers. The detailed description of the synthesis and characterization of the PEI block is presented in SI (Section 1). The major parameters for the obtained oligomer are also shown in SI (Table S1). In brief, to obtain the polyester, IsoCl was reacted with EG through the Schotten–Baumann reaction between acid chloride and hydroxyl functionalities of the monomers (Figure S1, SI).[27−29] We employed a classical Carothers approach to regulate the molecular weight and the chemical nature of the polyester end groups during polycondensation using stoichiometric imbalance.[30,31] The PEI synthesis was conducted by a combination of solution and melt polymerization following the procedure previously employed by us to obtain PFPE-based oligomeric polyesters.[10] According to the TGA (Figure S4, SI), the obtained oligomers have ~20% lower-molecular-weight fraction, which is thermally stable until ~200 °C, whereas the major PEI fraction withstands higher temperature (>300 °C). The major fraction of the product had the decomposition temperature (T_d) of around 388 °C. The GPC results indicated that PEI oligomers with a weight-average molecular weight (M_w) of 1564 g/mol and polydispersity index (PDI) of 2.8 were obtained. We associate the relatively high PDI with the presence of lower-MW oligomers in the samples. On the basis of M_w, we estimated that the number of repeating units for PEI was ~7.

The thermal transitions of the PEI oligomer were studied by DSC (Figure S5, SI). We found that the oligomer is an amorphous material with a midpoint glass-transition temperature (T_g) of −5 °C. The result indicates that PEI chains possess a high chain mobility/diffusivity at and above room temperature. This behavior supports the migration of targeted FOPBs to the surface of thermoplastic materials. The polyester structure was examined with ATR-FTIR (Figure S6, SI). The results were analyzed using readily available spectral databases for organic compounds.[32] IR spectra confirmed that the targeted PEI oligomers were obtained.

FOP Blocks. The general schematic for synthesis of FOP blocks is depicted in SI (Figure S2). Table S1 (SI) presents the major parameters for the synthesized macromolecules. For the block synthesis, we used the same chemical procedures as for the synthesis of the PEI oligomer. Two different semitelechelic oligomeric blocks end-terminated with (i) one hydroxyl and one C_4F_9–PFPE– end group (FOP-1) and (ii) one hydroxyl and one C_6F_{13}– end group (FOP-2) were obtained. The detailed description of the synthesis and characterization of FOP blocks is presented in SI (Section 1). The synthesized FOPs were analyzed with TGA (Figure S7, SI). The TGA measurements indicated that the higher-molecular-weight oligomer fractions were ~82 and ~88% for FOP-1 and FOP-2, respectively. TGA results also showed that FOP oligomers of higher molecular weight have T_d above 400 °C. M_w for the oligomers was on the level of 4000−5000 g/mol (Table S1, SI). The estimated numbers of repeating units for FOP-1 and FOP-2 are ~8 and ~7, respectively. Consequently, the weight percent of the fluorinated end segments is quite similar and is about 11% for FOP-1 and 8% for FOP-2. ATR-FTIR analysis was performed to identify the major functional groups in the obtained FOPs (Figure S8, SI). In general, IR spectroscopy confirms that the fluorinated polyester oligomers were synthesized successfully. DSC analysis showed that FOPs are semicrystalline materials having both a T_g and melting temperature, T_m (Figure S9, SI). T_g values for FOP-1 and FOP-2 are −35 and −22 °C, respectively. We attribute the difference in T_g to the chemical composition of FOP end groups. Owing to the oxygen atoms, the C_4F_9–PFPE– tails in FOP-1 are more flexible than C_6F_{13}– tails in FOP-2.[33] Thus,

DOI: 10.1021/acs.langmuir.8b02628
Langmuir 2018, 34, 12934−12946

the T_g for FOP-1 is lower than that of FOP-2. It is necessary to point out that both FOPs have the same melting temperature of ~47 °C because both materials possess the same crystalizing repeating unit.

FOPB Copolymers. The chemical schematic for the synthesis of FOPB-1 (copolymer with C_4F_9−PFPE− end groups) and FOPB-2 (copolymer with C_6F_{13}− end groups) via the Schotten−Baumann reaction in melt is displayed in Figure S3, SI. The detailed description of FOPB synthesis and characterization is reported in SI (Section 1). The characteristics of the obtained block copolymers and their chemical structure are presented in SI (Table S2 and Figure 2, respectively). According to the TGA results (Figure S10, SI), the major component (>97%) of the obtained FOPBs corresponds to the higher-molecular-weight product having T_d above 300 °C. This indicates that FOPB-1 and FOPB-2 copolymers have significant thermal stability irrespective of the end groups. ATR-FTIR analysis supported the proposed chemical structure of FOPB because the major functional groups of FOPBs are present in the IR spectra (Section 1 and Figure S11, SI). ^{19}F NMR spectroscopy further confirmed synthesis of the targeted FOPBs (Section 1 and Figures S12 and S13, SI). The MW and PDI of FOPBs are on the level of 8000−10 000 g/mol and 2−3, respectively. On the basis of the structure of end groups; M_w; and number of repeating units for PEI, FOP-1, and FOP-2 blocks, we estimated that the atomic concentration of fluorine in the block copolymer chain is practically the same: 25% for FOPB-1 and 24% for FOPB-2.

DSC analysis was performed to determine T_g and T_m for FOPBs (Figure 3). The results showed that FOPBs are semicrystalline materials because both T_g and T_m were detected. For FOPB-1 and FOPB-2, T_m values are 46 and 48 °C, whereas midpoint T_g values are −18 and −16 °C, respectively. DSC data suggested that the influence of end groups on the position of copolymer thermal transitions is not significant. In general, the glass-transition temperature of copolymers is significantly higher than the one for the FOP blocks, indicating significant influence of the middle PEI block on the transition. However, the melting temperature is not influenced by the PEI block. In general, we anticipated that the relatively low T_g and T_m have to facilitate migration of the FOPB additives to the boundary of thermoplastic polymer materials and thus increase their water and oil repellency.

Morphology of FOPB/PET Films. PET films with different concentrations of FOPBs were prepared by dip coating from FOPB/PET solution. The films were divided into two groups: (i) the films from the first group were dried at ambient conditions and (ii) the films from the second group were first dried and then annealed at 140 °C for 3 h under vacuum. The annealing temperature was selected to be above the FOPBs' thermal transitions and the T_g of PET (70−80 °C[34,35]), yet below the melting temperature of PET (250−260 °C[34,35]). In practical applications, only films with a low concentration of fluorine species can be employed; therefore, we prepared polymer films containing 1, 2, 5, and 10% of FOPBs to study the effect of copolymer content on the surface morphology.

AFM imaging was used to investigate the micro-/nanoscale morphology of the films before (Figures 4 and S14, SI) and after the annealing (Figures 4, S15, and S16, SI) treatment for FOPB/PET films possessing different amounts (1−10%) of the fluorinated copolymers. Figures 4 and S14 show that the smooth polymer films were fabricated from FOPB/PET solutions without visible crystal formation. It is apparent that PET and FOPBs are to some extent immiscible and phase-separated (dark) domains of FOPBs are clearly visible in a (bright) PET matrix on the AFM images. Figures 4 and S15 show that the annealing treatment has a significant effect on the surface morphology because the crystalline structures are formed within FOPB/PET films. We also note that the phase separation of FOPBs is not clearly observed for the annealed films on AFM topographical images. Thus, it is possible that as a result of annealing FOPB dissolves in the PET matrix. In an alternative scenario, FOPB spreads over the PET surface, forming a continuous layer (as a lower-surface-energy component for thermodynamical reasons[33]).

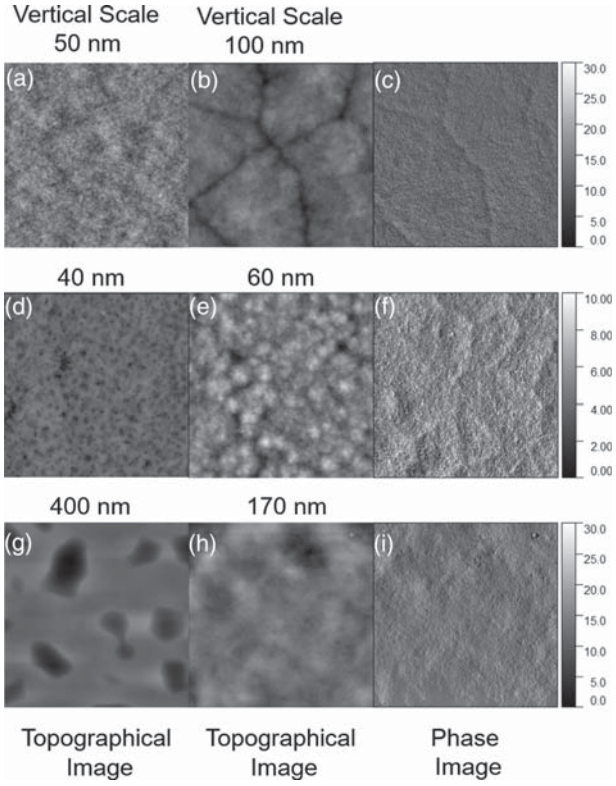

Figure 4. AFM (10 μm × 10 μm) images of polymer films of pure PET (a−c), 10 wt % FOPB-1/PET films (d−f), and 10 wt % FOPB-2/PET (g−i) films. Topographical images before annealing (a, d, g) and after annealing (b, e, h). Phase images of the annealed films (c, f, i). The scale is in degrees.

To clarify this matter, we have determined thermal transitions of the annealed (at 140 °C for 3 h) FOPB/PET blends (Figures S17 and S18, SI). The transitions were compared to the ones observed for pure PET and FOPBs materials processed under the same conditions. The major focus was to understand if FOPBs have some level of miscibility with the PET matrix. To this end, we followed the PET melting transition, which does not overlap with T_g and T_m of FOPBs. If at least the partial miscibility of PET and FOPB is present, it has to significantly decrease the melting temperatures of PET.[33] However, data for the FOPB/PET blends (Section 12 and Table S3, SI) shows that there is no significant and systematic decrease in T_m of the PET matrix with addition of FOPBs. For the blends containing 80% of FOPBs, it was found that T_m for the fluorinated block copolymer is not influenced by the presence of PET phase as

DOI: 10.1021/acs.langmuir.8b02628
Langmuir 2018, 34, 12934−12946

well (Figures S17 and S18, SI). Therefore, the polymer materials are practically immiscible. Since the copolymers cannot be accommodated in the PET matrix and have lower surface energy, we suggest that upon annealing FOPBs spread over the boundary of the film and form a continuous layer. In fact, AFM phase images (Figures 4 and S16), which are particularly sensitive to heterogeneity of surface composition,[36] do not show that the surface layer is discontinuous and partially covering the film surface. On the basis of the AFM and DSC results, we assume that after the annealing step practically all of the surface of the FOPB/PET films is covered with the nanoscale copolymer layers.

Thermodynamics of FOPB Layer Formation. Our study of the FOPB/PET film morphology indicates that FOPB is immiscible with PET and presumably forms a nanoscale layer covering the exterior of the film. On the basis of thermodynamical conditions of minimization of surface energy, we evaluated the capability of the FOPB layer to possess brushlike structures, in which the PEI block segregated to the PET surface (Figure 2b). To this end, we estimated surface energies and their (polar and dispersive) components for the PEI block, FOP blocks, and PET as well as determined the interfacial energies in the system (Section 13 and Table S4, SI) using algorithms reported elsewhere.[33,37−39]

We then considered two border situations (A and B) for the FOPB layer arrangement on the PET surface. In case A, the layer has PEI blocks exposed to the layer exterior, whereas FOP blocks are segregated to the PET boundary (Figure 5a). In scenario B (FOPB brush formation), FOP chains are located on the surface, whereas PEI is in contact with the PET surface (Figure 5b). In the first arrangement, the change in the Gibbs energy can be approximated using eq 1 (Section 13, SI)

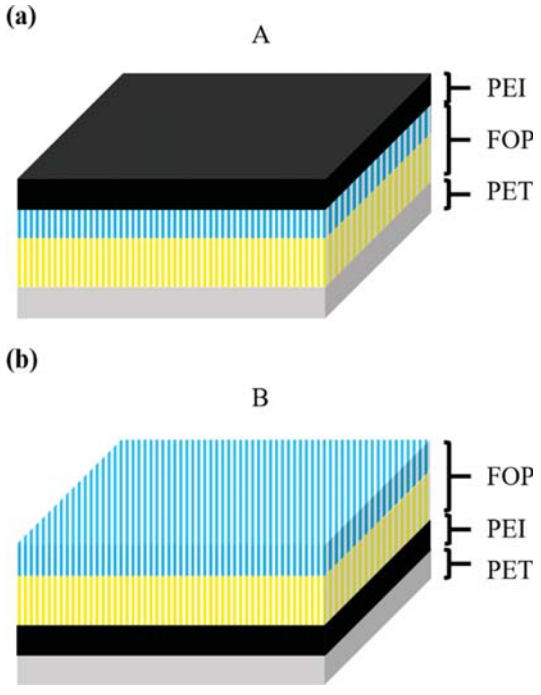

Figure 5. Schematic illustration of the two border situations for the FOPB monolayer arrangement on the PET surface: (a) PEI is exposed to the exterior, whereas FOP is located on the PET surfaces; (b) PEI is in contact with PET, whereas FOP is exposed to the exterior.

$$dG_1 = -\gamma_{FOP} + \gamma_{PEI} + \gamma_{FOP\text{-}PEI} - \gamma_{PET} + \gamma_{PET\text{-}FOP} \quad (1)$$

where γ_{FOP} is the surface energy of FOP, γ_{PEI} is the surface energy of PEI, $\gamma_{FOP\text{-}PEI}$ is the interfacial tension for FOP-PEI, γ_{PET} is the surface energy of PET substrates, and $\gamma_{PET\text{-}FOP}$ is the interfacial tension between PET substrates and FOP. For the second arrangement, the change in Gibbs energy equation can be estimated using eq 2 (Section 13, SI)

$$dG_2 = -\gamma_{PEI} + \gamma_{FOP} + \gamma_{FOP\text{-}PEI} - \gamma_{PET} + \gamma_{PET\text{-}PEI} \quad (2)$$

where $\gamma_{PET\text{-}PEI}$ is the interfacial tension value for PET substrates and PEI. Using data from Table S4, SI, the changes in Gibbs free energy of the layer arrangements were calculated to be −21 mN/m (FOPB-1) or −24 mN/m (FOPB-2) for arrangement A and −59 mN/m (FOPB-1) or −59 mN/m (FOPB-2) for arrangement B. It is evident that the lowest free energy for the layer formation is given by arrangement B, where PEI is segregated to the PET surface and FOP blocks are positioned at the external interface. Therefore, from the thermodynamic point of view, the formation of the FOPB brushlike layer on the PET surface is favorable. This is the preferential arrangement for the applications targeted here, where fluorine entities are needed at the polymer boundary to minimize its surface tension.

Wettability of Solvent-Cast FOPB/PET Films. We evaluated the degree of hydrophobicity and oleophobicity of solvent-cast (no annealing) FOPB/PET films by measuring the static contact angle of water (WCA) and hexadecane (HCA). It was shown experimentally that liquids with bulky molecules like hexadecane are suitable for contact angle measurements to characterize energetics of fluorinated polymer surfaces.[40,41] Prior to the CA measurements, we evaluated the copolymer solubility in the wetting liquids and found out that FOPBs are not soluble in water and hexadecane. In addition, a pure PET film was also prepared to identify its wettability with water and oil (hexadecane). The CAs were measured after the films were stored at ambient conditions for 16 h after the fabrication. The wettability results are presented in Figure 6a. It is obvious that the pure PET film is nearly completely wettable with hexadecane (HCA < 5°) and partially wettable with water (WCA ≈ 58°). We found that a small amount of the fluorinated triblock copolymers incorporated into PET resulted in a significant increase in the values of both WCA and HCA. For instance, the WCA and HCA were increased for the films containing 1−2% of FOPBs up to the level of 70−80 and 30−50°, respectively. In general, the wettability of the films decreased with the FOPB content as more fluorinated copolymer is present on the film surface. For the films containing 10% of FOPBs, the WCA and HCA are 80−90 and 55−65°, respectively.

Our preceding studies on wettability of PET films containing PFPE-based oligomeric polyesters indicated that the solvent-cast films are not at equilibrium and the enrichment of the film surface with the oligomeric polyesters continues for several days.[10] Therefore, to study if surface enrichment of triblock copolymers varied with the storage time, we conducted CA measurements on the films containing 5% FOPB-1 and FOPB-2 as a function of time. In parallel, AFM imaging of the films was also conducted (data not shown). In general, we found that there was no significant change in the FOPB/PET surface morphology imaged with AFM as a result of storage.

The wettability results are displayed in Figure 6b. Indeed, the migration of FOPB to/over the film boundary continues

DOI: 10.1021/acs.langmuir.8b02628
Langmuir 2018, 34, 12934−12946

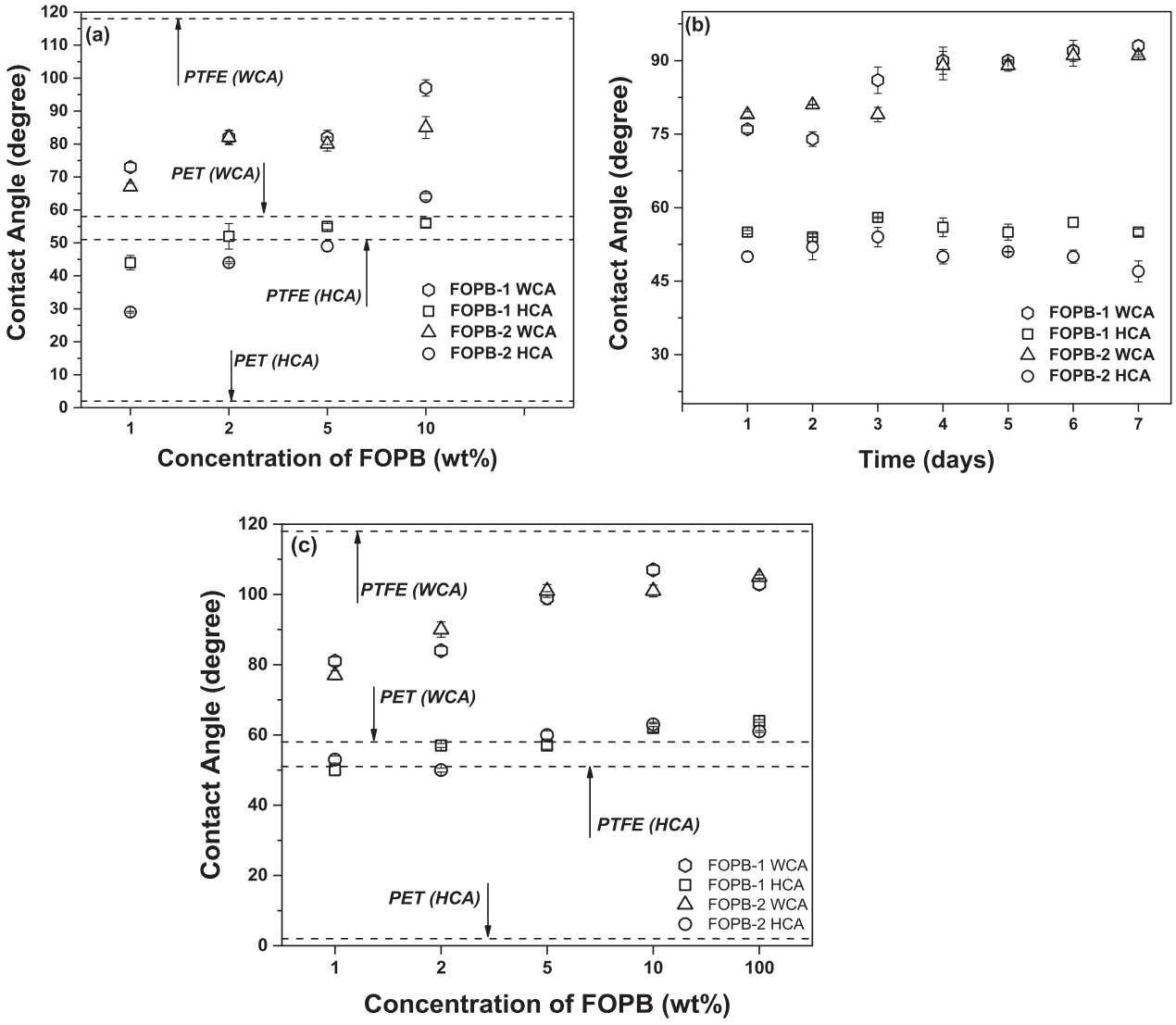

Figure 6. WCA and HCA for FOPB/PET films. (a) CAs for films of different FOPB contents before annealing. (b) CAs for 5% FOPB/PET films stored for different times. (c) CAs for the annealed FOPB/PET films having different FOPB contents. Contact angles for PET and PTFE are given for comparison.

for up to 6−7 days, as indicated by a significant change in WCA that increased by ∼10° after 7 days of storage. We note that HCA practically does not change with the storage time. Therefore, it appears that WCA is more sensitive to the density (or thickness) of the FOP monolayer covering the PET phase. The results suggest that the size of the wetting liquid plays a critical role in wettability. Indeed, based on the molecular weight and chemical structure, the size of water molecule is about an order of magnitude smaller than that of hexadecane. Specifically, the molecular volumes for water and hexadecane at 20 °C are 30 and 458 Å^3, respectively.[42] Therefore, water can penetrate to a greater degree through the layer of fluorinated oligomer and contact the PET matrix when compared with hexadecane.

It is necessary to point that we did not observe a clear difference in the wettability of FOPB-1/PET and FOPB-2/PET possessing different end groups. In fact, for certain block copolymer concentrations, WCA and/or HCA of FOPB-1/PET is higher than that of FOPB-2/PET. However, for films of a different block copolymer content, the opposite result was found. In general, the wettability experiments with solvent-cast films indicated that a significant amount of time is needed for films to approach equilibrium and to reach higher levels of water and oil repellency. It is obvious that for practical applications annealing of the films is necessary. Moreover, in an industrial setting, the thermoplastic materials are fabricated at elevated temperatures via melt processing. Therefore, our further study focused solely on the annealed FOPB/PET films.

Wettability of Annealed FOPB/PET Films. Figure 6c shows the results of WCA and HCA measurements for the FOPB/PET films annealed at 140 °C for 3 h. For the sake of comparison, we also conducted measurements for (the prepared and annealed at the same conditions) pure PET and FOPBs films. In general, the thermal treatment significantly increases WCA and HCA in comparison with solvent casting. It appears that elevated temperatures support the migration of the FOPB over the area on the film surface occupied by the PET matrix and approached the saturation limit. In addition, as demonstrated by AFM imaging, intensive crystallization of PET occurs at this temperature. We suggest

DOI: 10.1021/acs.langmuir.8b02628
Langmuir 2018, 34, 12934−12946

that densification (shrinkage) of the PET phase caused by the crystallization can also support the migration of FOPB macromolecules to the film surface.

There is a significant dependence of CAs on the concentration of the fluorinated copolymers in the FOPB/PET films. The WCA for FOPB-1/PET films increased from 81 to 107° as FOPB-1 content increased from 1 to 10%, and the HCA of the films increased from 50 to 62° with the FOPB-1 concentration. A similar scenario is observed with FOPB-2/PET films, where the WCA increased from 77 to 101° as the concentration of FOPB-2 increased from 1 to 10%. The HCA was also increased from 53° to the level of 63°. It is necessary to point out that wettability of the FOPB/PET films containing 10% of the copolymer is virtually the same as wettability of pure (100%) annealed FOPB films. This result indicates that practically all surface of the FOPB/PET film is "screened" with the copolymers from the wetting liquids.

We compared the wettability of FOPB/PET films with the wettability of poly(tetrafluoroethylene) measured by us using the same method as for FOPB/PET films. The WCA and HCA for PTFE were measured as 118 and 51°, respectively, which correlated well with the values in the scientific literature.[43,44] It was found out that the highest WCA for annealed FOPB/PET films is on the level of 100° and is reached at 5% copolymer content, which is relatively lower than that of PTFE. However, with addition of just 1% of FOPBs to PET, the oil repellency of the films is on the same level as that of PTFE. The oil repellency of FOPB/PET films is higher than that of PTFE when 2% of FOPB-1 or 5% of FOPB-2 is added to the PET matrix. It is necessary to highlight that at practically important concentrations (≤5%) the water and oil repellency of the films containing C_4 material (FOPB-1 with C_4F_9−PFPE− tails) is on the level of that of the films having C_6 material (FOPB-2 with C_6F_{13}− tails).

We also compared the water/oil repellency of the annealed PET films modified with FOPB-1 (Figure 2c) and the repellency of the annealed films modified with PFPE-based oligomeric polyester of the chemical structure shown in Figure 1c. The synthesis/structural characteristics of the FOP and wettability of the FOP/PET films are published elsewhere.[10,45] The structures of FOPB-1 and FOP are quite similar and differ only by the presence of the short PEI middle block in the FOPB macromolecule. However, owing to the PEI block, the copolymer is capable of forming brushlike structures (Figure 2b), whereas FOP can only spread over the surface (Figure 1b). The measured WCAs/HCAs for FOP/PET films containing 5 and 10% of the fluorinated polyester are 84/45 and 91/48°, respectively. These values are significantly (10−20°) lower than the ones observed for the FOPB-1/PET films having the same content of fluorinated macromolecules (Figure 6c). The obtained results indicated the clear superiority of the triblock copolymer system in terms of water and oil repellency of the modified thermoplastic polymer films.

Finally, we compared the wettability of the annealed FOPB/PET films with the published results on wettability of PET modified with the addition of perfluoropolyether-based materials. For instance, Pilati et al.[46] reported on water contact angle of PET modified with the poly(ε-caprolactone)−(perfluoropolyether)−poly(ε-caprolactone) triblock copolymer, PCL−PFPE−PCL. It was found that at 5 wt % loading the static contact angle for the modified PET was ∼87°. It is evident that water repellency of the 5% FOPB/PET film is significantly better than the one for the PET modified with PCL−PFPE−PCL. The oil repellency for PET modified with PCL−PFPE−PCL is not reported in the scientific literature. However, the advancing hexadecane contact angle for the 100% PCL−PFPE−PCL copolymer film is reported as 67°.[11] This value is quite close to the value of hexadecane static contact angles measured by us for the pure annealed FOPB films (64° for FOPB-1 and 62° for FOPB-2).

Estimation of Surface Area of PET Screened with FOPBs. Our thermodynamic estimations indicate that for the equilibrated FOPB/PET film all of the surface has to be covered with the layer of fluorinated copolymer. The AFM phase imaging and contact angle measurements (especially HCA) also clearly indicate that the surface of the film is occupied with the fluorinated copolymers. Therefore, the value of the contact angles is controlled by the thickness of the layer and ability of the FOPB macromolecules to screen the PET phase from the probing liquids. We estimated the effective surface area of PET shielded from the wetting liquids by the fluorinated copolymer using the classical Cassie−Baxter model (eq 3).[47,48] The model describes the apparent contact angle of a liquid ($\theta_{PET/FOPB}$) on a composite surface when the surface is not completely wetted by the liquid droplet

$$\cos\theta_{PET/FOPB} = f_{FOPB}\cos\theta_{FOPB} + f_{PET}\cos\theta_{PET} \quad (3)$$

where θ_{FOPB} and θ_{PET} are experimentally determined Young's contact angles of a liquid on pure (100%) FOPB and PET surfaces, respectively. f_{FOPB} and f_{FOPB} are surface area fractions of the component surfaces. From experimentally measured contact angles for the annealed FOPB/PET films ($\theta_{PET/FOPB}$), we calculated the surface fraction of the PET surface screened from the wetting liquids with FOPBs using eq 3. The results are presented in Table 1 and indicate that FOPBs readily segregated to the surface and effectively shielded it from the wetting liquids. We noted that FOPB-1 is better for shielding surfaces from hexadecane than from water, especially with low (1 and 2%) concentration in PET films. The same phenomenon is observed with PET films with addition of 1% FOPB-2. We reiterate here that the reason behind this observation is difference in the size of the probe liquid molecules. Therefore, more dense FOPB layers are needed to screen the PET phase from the smaller water molecules. Indeed, the difference disappears at higher concentrations of FOPBs. With 10% load, the PET material is practically fully screened with FOPBs.

Table 1. Apparent Surface Area of the Annealed FOPB/PET Films (f_{FOPB}), Which Is Screened Effectively by Fluorinated Chain Segments

polymer films	FOPB content (wt %)	f_{FOPB} from WCA	f_{FOPB} from HCA
FOPB-1/PET	1	0.49	0.7
	2	0.55	0.89
	5	0.89	0.89
	10	1	1
FOPB-2/PET	1	0.39	0.7
	2	0.68	0.65
	5	0.91	0.9
	10	0.92	0.98

XPS-Based Analysis of FOPB/PET Films. To further investigate the FOPBs localization on the boundary of the

DOI: 10.1021/acs.langmuir.8b02628
Langmuir 2018, 34, 12934−12946

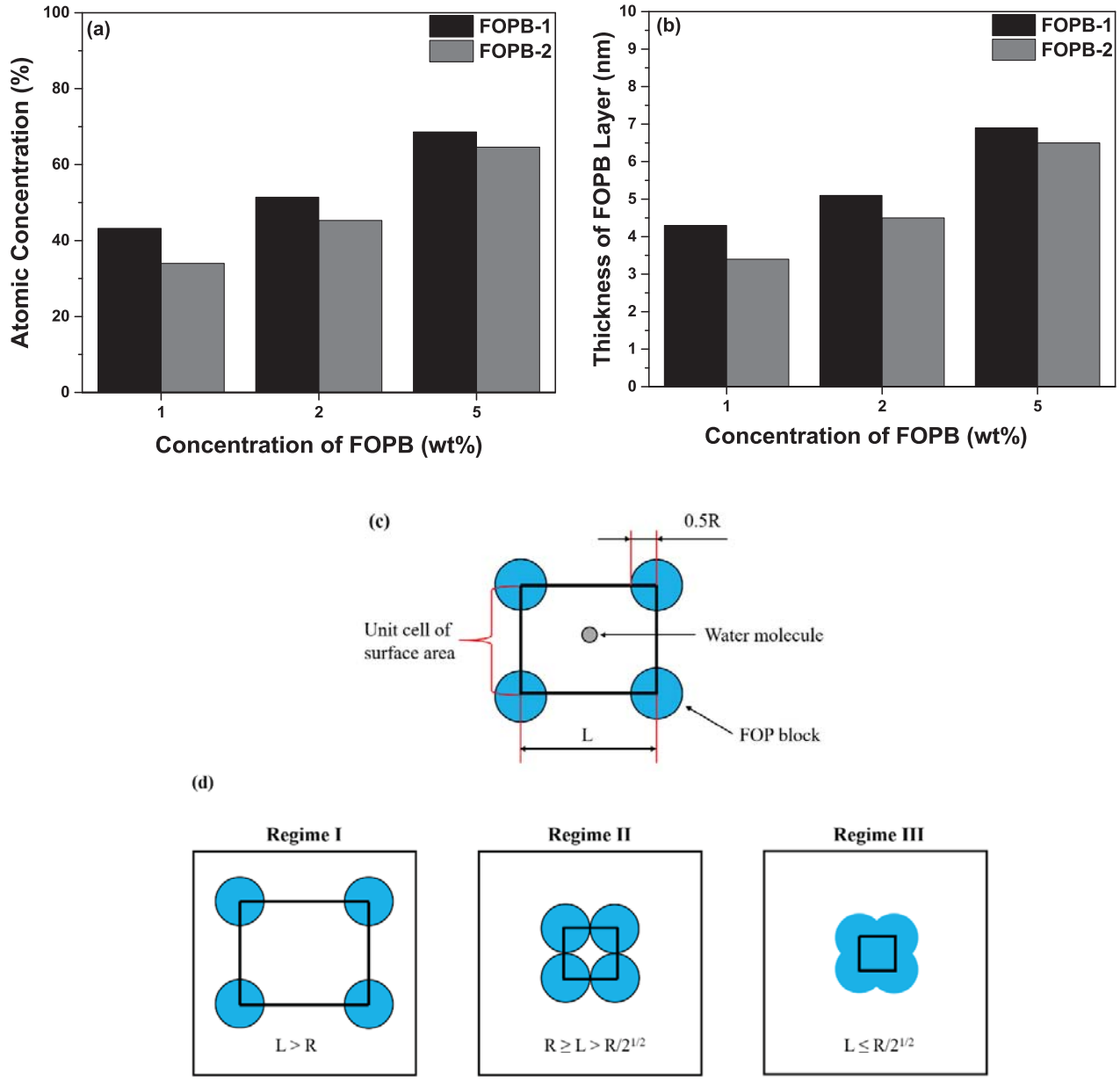

Figure 7. Atomic concentration of FOPB within 10 nm top layer (a) and the effective thickness of the FOPB layer on the surface (b) of the annealed FOPB/PET film as a function of FOPB concentration in the blends. A geometric two-dimensional model of surface coverage by the FOP chain: (c) radius of the disc is equal to the radius of gyration of the FOP brushes and (d) mathematical demonstration of three different regimes for FOP surface coverage.

FOPB/PET film, we conducted XPS analysis for the annealed films with different copolymer concentrations (1, 2, and 5%). In this study, samples were analyzed at an incident angle of 90°, where the detector line of sight was normal to the film. Therefore, the corresponding sampling depth from the air/film boundary was around 10 nm.[20,49] XPS survey spectra of the top 10 nm layer of FOPB/PET films primarily possess three characteristic peaks: F 1s, O 1s, and C 1s. The F 1s signal was from the fluorinated copolymer. The O 1s and C 1s peaks were from both FOPBs and PET polymers. The XPS data is displayed in SI (Tables S5 and S6). The atomic concentration of fluorinated triblock copolymer segments in the topmost 10 nm layer was calculated using the experimental F/O ratio from the survey spectra and not F/C ratio to avoid possible carbon-based contaminates. The following equations were applied[10,50]

$$\left(\frac{\mathrm{F}}{\mathrm{O}}\right)_{\mathrm{XPS}} = \frac{X_{\mathrm{FOPB}}F_{\mathrm{FOPB}}}{X_{\mathrm{FOPB}}O_{\mathrm{FOPB}} + (1 - X_{\mathrm{FOPB}})O_{\mathrm{PET}}} \quad (4)$$

$$X_{\mathrm{FOPB}} + X_{\mathrm{PET}} = 1 \quad (5)$$

where X_{FOPB} and X_{PET} are the atomic concentrations of FOPBs and PET within the top layer, respectively. F_{FOPB} and O_{FOPB} are the fluorine and oxygen atomic concentrations in the fluorinated copolymers obtained from spectra of 100% FOPB films (Tables S5 and S6, SI). O_{PET} is the oxygen atomic concentrations in the PET polymer. Because hydrogen atoms are not detectable in our XPS experiment, O_{PET} was calculated

DOI: 10.1021/acs.langmuir.8b02628
Langmuir 2018, 34, 12934−12946

using only carbon and oxygen present in the PET structure. The concentration of the fluorinated copolymer within 10 nm layer from the air/film interface (calculated by eq 4) is presented in Figure 7a. The results clearly indicate that the FOPB content in the topmost layer is increasing with FOPB concentration and is more than an order of magnitude higher than that in the film bulk. It appears that the exterior of the FOPB/PET films is extensively enriched with the fluorinated copolymers.

Structural Characteristics of FOPB Layers. Our assumption of the annealed FOPB/PET film structure is based on the experimental results described in detail above and summarized here. First, DSC results for FOPB/PET mixtures have clearly indicated that there is no miscibility between the polymers. Therefore, there is no dissolution of the copolymer in the PET matrix upon annealing. Second, according to the wettability results, the surface of the FOPB/PET films is significantly enriched with the fluorinated copolymers. In fact, hexadecane (large molecule) contact angles of the FOPB/PET films are quite close to the contact angles measured for pure FOPB films and ∼10 times higher than HCA observed for the pure PET film. XPS measurements are in accord with the wettability data, indicating that the concentration of FOPBs within 10 nm layer from the air/film interface is more than an order of magnitude higher than that in the "as-prepared" film bulk. In addition, AFM phase imaging of the annealed FOPB/PET films has indicated that a uniform FOPB layer is formed over the semicrystalline FOPB/PET film. Finally, from the thermodynamic point of view, the formation of the FOPB brushlike layer on the PET surface is favorable.

As a first approximation, we have used the coarse grain model describing the top 10 nm of the film exterior probed with XPS as a two-layered system, where the FOPB layer is positioned on the top of the PET one. Within this model, we determined the effective thickness of the FOPB layers by considering the thickness of the layer to be directly proportional to the atomic concentration of FOPB within 10 nm of the surface and assumed that the density of FOPB and PET is 1.5 g/cm^3. The value of 1.5 g/cm^3 was selected based on known values of PET[34] (amorphous 1.34 g/cm^3, crystalline 1.52 g/cm^3) and PFPE[51] (1.8−1.9 g/cm^3) densities. Results are presented in Figure 7b. The thickness of the layer is on the level of 3−7 nm depending on FOPB concentration.

The topmost 10 nm layer of the film accessed with XPS constitutes about 3% of the total (300−350 nm) film thickness (volume). Therefore, on the basis of XPS results, we can estimate the atomic concentration of FOPB remaining in other 97% of the film using the following simple relationship: (FOPB atomic fraction in the entire film − FOPB atomic fraction in the top 10 nm layer × 0.03)/0.97. If we consider that the weight fractions are equal to the atomic fractions, the concentrations of FOPB remaining in other 97% of the film are on the level of 0, 0.05, and 3% for FOPB/PET films with "as-prepared" FOPB contents of 1, 2, and 5%, respectively. One can clearly see that for the film possessing 1 and 2% of the fluorinated copolymer most of FOPB is migrated to the topmost film layer.

We compared the FOPB layer thickness with dimensions of the FOPB macromolecules. To this end, we estimated the root-mean-square end-to-end distance (R) of the macromolecular chain. We calculated the upper border value of R size by assuming the same scaling relationships as for oligomeric PET, which is less flexible than FOPB, using eq 6:[10,52]

$$R = 0.04(M_w)^{0.57} \quad (6)$$

where M_w is the weight-average molecular weight of FOPB. Then, the lower border end-to-end distance was also estimated using eq 7 for perfluoropolyethers, which are more flexible than FOPBs[10,53]

$$R = 0.056(M_w)^{0.5} \quad (7)$$

Our estimations indicated that R values are 6−8 nm for FOPB-1 and 5−7 nm for FOPB-2. Therefore, the thickness of copolymer layers is ∼0.5 FOPB monolayer for the films with 1% of FOPB. The thickness increased to ∼1 monolayer for the films having 5% of the fluorinated copolymer.

Our thermodynamic estimations point out that the macromolecules in the layer have to be organized in a brushlike structure, whereas PEI blocks are segregated to the PET surface. In this structure, FOP blocks are anchored by the one end to the surface, whereas another C_4F_9−PFPE−/C_6F_{13}− fluorinated end is exposed to the air (Figure 2b). We estimated parameters of the brush layer using relationships developed for polymer-grafted layers. Specifically, we calculated the chain density of FOP brushes, the surface coverage of FOP brush, and average distance (L) between FOP chains in the brush layer (Section 15, SI). The calculated parameters for the FOPB layers are presented in Table S7. To better understand how the parameters are related to the size of FOP blocks, we determined (using eq 7) that the end-to-end distances for FOP-1 and FOP-2 are practically the same and are between 4 and 5 nm. From R and L, it is possible to evaluate the degree of the overlap between FOP chains in the brushlike layer using the straightforward geometrical model described elsewhere (Figure 7c,d).[54−56] It is obvious that the higher degree of overlap is directly related to the higher capability of the FOP layer to screen the PET matrix from the wetting liquids.

There are three different regimes to be considered for surface shielding effects within the geometrical model. In regime I ($L > R$), FOP chains are spaced out, do not overlap, and do not screen the surface effectively. However, when the FOP chain density is increased, the chains start to overlap and transit to regime II ($R \geq L > R/2^{1/2}$). In regime II, the chain density is not sufficient to cover the whole surface area. In regime III ($L \leq R/2^{1/2}$), the chain density is sufficient to screen the surface completely. There is no open surface in the case of regime III. A comparison of R (∼4.5 nm) and $R/2^{1/2}$ (∼3 nm) values for FOPs with L values presented in SI (Table S7) showed that all of the copolymer layers studied here follow regime III. However, even when the surface is fully covered with FOP chains only, values of FOP block chain density $\sum$ on the level of 1 chain/nm^2 (5% FOPB/PET films) are effective in screening the PET material from both water and hexadecane. At these values of $\sum$, thickness of the FOPB layer is somewhat higher than the end-to-end distance of FOP blocks and, therefore, the FOP blocks stretch away from the surface and populate the surface with low energy C_4F_9−PFPE− and C_6F_{13}− end segments.

Surface Energy Estimation. Surface energy (σ) was also estimated to further elucidate the characteristics of the FOPB/PET films. This was calculated from WCA and HCA data using the Owens−Wendt method (Section 16, SI).[48,57−61] This method is one of the most used to determine the surface

DOI: 10.1021/acs.langmuir.8b02628
Langmuir 2018, 34, 12934−12946

energy of polymer surfaces and is based on principal assumption that the surface energy is a sum of two components: dispersion and polar. Other major approaches that can be used for this purpose are Oss−Chaudhury−Good and Newman methods.[58,62] It is necessary to point that determination of surface energy of polymer surfaces is not a fully solved problem and every method has its benefits, limitations, and shortcomings. The energies determined using different methodologies are not absolutely equal to one another.[58,62,63] Therefore, only the results produced by the same method with the use of identical wetting liquids may directly be compared.

Figure 8 shows that the PET film possesses a relatively high surface energy around 46 mN/m. However, when only a small amount of FOPB is added to PET, the film surface energy is significantly decreased. For example, at a concentration of 2%, the surface energies are 25 and 23 mN/m for FOPB-1 and FOPB-2, respectively. It is necessary to highlight that all films with 2% addition shows σ just 20% above that of PTFE (σ_{PTFE} = 18.5 mN/m). Furthermore, at 5% concentration, all films have a surface energy practically equal to σ_{PTFE}. For the films with 10% of FOPB, σ_1 and σ_2 are equal to 15 and 17 mN/m, respectively. Namely, both FOPB-1 and FOPB-2 with 10% load have lower surface energy than that of PTFE. It is also noted that C_4 material (FOPB-1) has a surface energy value quite similar to that of C_6 polymer (FOPB-2) at all concentrations.

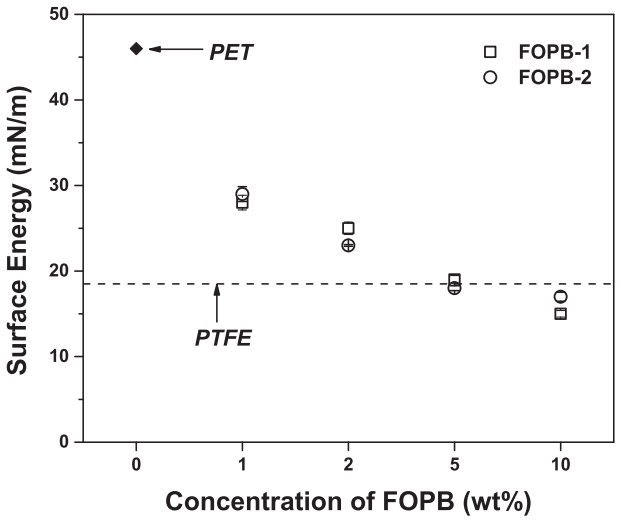

Figure 8. Surface energy of FOPB/PET films after annealing. Surface energies for PET and PTFE are given for comparison.

Addition of FOPB to Other Thermoplastic Materials. To demonstrate the applicability of our surface modification approach utilizing FOPBs to other than PET engineering thermoplastics, we prepared FOPB/nylon-6 and FOPB/PMMA films. The FOPB content in the films was 5%. The films were annealed at 140° for 3 h prior to the CA measurements. The obtained wettability and surface energy results are presented in Table 2. It is obvious that both pure nylon-6 and PMMA are partially wettable with water and nearly completely wettable by hexadecane. The incorporation of FOPB in the thermoplastics dramatically increased HCA of the surface. We note that the HCA for FOPB-1/nylon-6 and FOPB-1/PMMA increased from 1−5 to 72 and 88°, respectively. For FOPB-2, the same trend was observed as the HCA increased from 1−5 to 68° for nylon-6 and to 70° for PMMA. The WCA was also significantly increased with FOPB addition. The surface energy for annealed films was also estimated. Table 2 shows that both pristine nylon-6 and PMMA have a quite similar and relatively high surface energy at 37 and 35 mN/m, respectively. Conversely, at 5% FOPB/nylon-6 films, the surface energy is 24 and 23 mN/m for FOPB-1 and FOPB-2, respectively. For the films blended with PMMA, the surface energy for both FOPB-1 (9 mN/m) and FOPB-2 (13 mN/m) becomes much lower than that of PTFE (σ_{PTFE} = 18.5 mN/m). Without an additional study, we cannot offer a comprehensive explanation why FOPB/PMMA films have much lower surface energy than that of the FOPB/PET and FOPB/nylon-6 ones. However, we can conclude that the addition of FOPBs can decrease the surface energy of various engineering thermoplastics and not only PET.

CONCLUSIONS

FOPB materials, particularly the ones with four perfluorinated carbon atoms, can be employed as safer replacements to long-chain perfluoroalkyl substances. In fact, it was found that the macromolecules synthesized here, when added to industrial polymer (PET, nylon-6, and PMMA) films, readily migrate to the film surface and bring significant water and oil repellency to the thermoplastic boundary. The films reach the level of oil repellency and surface energy comparable to that of poly(tetrafluoroethylene), a fully perfluorinated polymer. The water/oil wettability of the PET films modified with FOPB-1 is lower than the wettability of the films modified with analogous PFPE-based polyester, which differs from FOPB-1 only by the absence of the short PEI middle block. We associate superiority of the triblock copolymers in achieving high water and oil repellency with their ability to form brushlike structures on polymer film surfaces. Finally, we established that FOPBs containing C_6F_{13}− and C_4F_9−PFPE− end groups demonstrate comparable level of water and oil repellency.

ASSOCIATED CONTENT

Supporting Information

The Supporting Information is available free of charge on the ACS Publications website at DOI: 10.1021/acs.langmuir.8b02628.

Synthesis of materials (Section S1); TGA data for PEI (Section S2); DSC data for PEI (Section S3); ATR-

Table 2. CAs and Surface Energies for Annealed 5% FOPB/Thermoplastic Films

	pure thermoplastic films			5% of FOPB-1 in the films			5% of FOPB-2 in the films		
materials	WCA (deg)	HCA (deg)	surface energy (mN/m)	WCA (deg)	HCA (deg)	surface energy (mN/m)	WCA (deg)	HCA (deg)	surface energy (mN/m)
nylon-6	72 ± 0.4	1−5	37 ± 0.1	83 ± 2.6	72 ± 0.3	24 ± 1.6	84 ± 1.8	68 ± 0.2	23 ± 1.1
PMMA	77 ± 2	1−5	35 ± 1.1	111 ± 1.2	88 ± 0.1	9 ± 0.3	109 ± 1.5	70 ± 0.2	13 ± 0.3

DOI: 10.1021/acs.langmuir.8b02628
Langmuir 2018, 34, 12934−12946

FTIR spectra of PEI (Section S4); TGA data for FOPs (Section S5); ATR-FTIR spectra of FOPs (Section S6); DSC data for FOPs (Section S7); TGA data for FOPBs (Section S8); ATR-FTIR spectra of FOPBs (Section S9); ^{19}F NMR data for FOPBs (Section S10); AFM topographical and phase images of pure PET and FOPB/PET films (Section S11); DSC data for annealed PET films and FOPB/PET blends (Section S12); calculation of surface tension and determination of FOPB layer formation (Section S13); XPS data for annealed FOPB/PET films (Section S14); calculation of structural parameters of FOPB polymer brush layer (Section S15); estimation of surface energy for FOPB/PET films (Section S16); references (Section S17) (PDF)

AUTHOR INFORMATION

Corresponding Author

*E-mail: luzinov@clemson.edu.

ORCID

Vladimir Tsukruk: 0000-0001-5489-0967

Igor Luzinov: 0000-0002-1604-6519

Notes

The authors declare no competing financial interest.

ACKNOWLEDGMENTS

The research reported was partially supported by the National Science Foundation via I/UCRC-1034979, EPSCoR OIA 1655740, and the Air Force Office for Scientific Research FA9550-17-1-0297. A.G. was supported by the National Science Foundation Graduate Fellowship. The authors gratefully acknowledge Kimberly Ivey (Clemson University) for her help and advice. Authors also thank Mykhailo Savchak (Clemson University) for the preparation of the images used in Figures 1, and 2.

REFERENCES

(1) Buck, R. C.; Franklin, J.; Berger, U.; Conder, J. M.; Cousins, I. T.; de Voogt, P.; Jensen, A. A.; Kannan, K.; Mabury, S. A.; van Leeuwen, S. P. J. Perfluoroalkyl and polyfluoroalkyl substances in the environment: Terminology, classification, and origins. *Integr. Environ. Assess. Manage.* **2011**, *7*, 513−541.

(2) Kissa, E. *Fluorinated Surfactants and Repellents*; Surfactant Science Series; Dekker: New York, 2001; Vol. 97, p 616.

(3) Soto, D.; Ugur, A.; Farnham, T. A.; Gleason, K. K.; Varanasi, K. K. Short-Fluorinated iCVD Coatings for Nonwetting Fabrics. *Adv. Funct. Mater.* **2018**, *28*, No. 1707355.

(4) Walters, K. B.; Schwark, D. W.; Hirt, D. E. Surface Characterization of Linear Low-Density Polyethylene Films Modified with Fluorinated Additives. *Langmuir* **2003**, *19*, 5851−5860.

(5) Conder, J. M.; Hoke, R. A.; de Wolf, W.; Russell, M. H.; Buck, R. C. Are PFCAs Bioaccumulative? A Critical Review and Comparison with Regulatory Criteria and Persistent Lipophilic Compounds. *Environ. Sci. Technol.* **2008**, *42*, 995−1003.

(6) Guo, J.; Resnick, P.; Efimenko, K.; Genzer, J.; DeSimone, J. M. Alternative Fluoropolymers to Avoid the Challenges Associated with Perfluorooctanoic Acid. *Ind. Eng. Chem. Res.* **2008**, *47*, 502−508.

(7) US Environmental Protection Agency. Long-Chain Perfluorinated Chemicals (PFCs) Action Plan, 2018. https://www.epa.gov/assessing-and-managing-chemicals-under-tsca/long-chain-perfluorinated-chemicals-pfcs-action-plan (accessed July 24, 2018).

(8) https://www.epa.gov/assessing-and-managing-chemicals-under-tsca/and-polyfluoroalkyl-substances-pfass-under-tsca (accessed July 24, 2018).

(9) Camaiti, M.; Brizi, L.; Bortolotti, V.; Papacchini, A.; Salvini, A.; Fantazzini, P. An Environmental Friendly Fluorinated Oligoamide for Producing Nonwetting Coatings with High Performance on Porous Surfaces. *ACS Appl. Mater. Interfaces* **2017**, *9*, 37279−37288.

(10) Demir, T.; Wei, L.; Nitta, N.; Yushin, G.; Brown, P. J.; Luzinov, I. Toward a Long-Chain Perfluoroalkyl Replacement: Water and Oil Repellency of polyethylene terephthalate (PET) Films Modified with Perfluoropolyether-Based Polyesters. *ACS Appl. Mater. Interfaces* **2017**, *9*, 24318−24330.

(11) Toselli, M.; Messori, M.; Bongiovanni, R.; Malucelli, G.; Priola, A.; Pilati, F.; Tonelli, C. Poly(ϵ-caprolactone)-Poly(fluoroalkylene oxide)-Poly(ϵ-caprolactone) Block Copolymers. 2. Thermal and Surface Properties. *Polymer* **2001**, *42*, 1771−1779.

(12) Lopez, G.; Ameduri, B.; Habas, J.-P. A Versatile Strategy to Synthesize Perfluoropolyether-Based Thermoplastic Fluoropolymers by Alkyne-Azide Step-Growth Polymerization. *Macromol. Rapid Commun.* **2016**, *37*, 711−717.

(13) Pilati, F.; Toselli, M.; Vallieri, A.; Tonelli, C. Synthesis of Polyesters-perfluoropolyethers Block Copolymers. *Polym. Bull.* **1992**, *28*, 151−157.

(14) Lopez, G.; Ameduri, B.; Habas, J. P. A Versatile Strategy to Synthesize Perfluoropolyether-Based Thermoplastic Fluoropolymers by Alkyne-Azide Step-Growth Polymerization. *Macromol. Rapid Commun.* **2016**, *37*, 711−717.

(15) Credi, C.; Levi, M.; Turri, S.; Simeone, G. Stereolithography of Perfluoropolyethers for The Microfabrication of Robust Omniphobic Surfaces. *Appl. Surf. Sci.* **2017**, *404*, 268−275.

(16) Jellali, R.; Paullier, P.; Fleury, M. J.; Leclerc, E. Liver and Kidney Cells Cultures in a New Perfluoropolyether Biochip. *Sens. Actuator, B* **2016**, *229*, 396−407.

(17) Toselli, M.; Pilati, F.; Fusari, M.; Tonelli, C.; Castiglioni, C. Fluorinated Poly(butylene terephthalate): Preparation and Properties. *J. Appl. Polym. Sci.* **1994**, *54*, 2101−2106.

(18) Fabbri, E.; Fabbri, P.; Messori, M.; Pilati, F.; Tonelli, C.; Toselli, M. Surface Modification of Unsaturated Polyester Resins with Perfluoropolyethers. *Polimery* **2004**, *49*, 785−789.

(19) Turri, S.; Barchiesi, E.; Levi, M. NMR of Perfluoropolyether Diols and Their Acetal Copolymers. *Macromolecules* **1995**, *28*, 7271−7275.

(20) Turri, S.; Radice, S.; Canteri, R.; Speranza, G.; Anderle, M. Surface Study of Perfluoropolyether−Urethane Cross-Linked Polymers. *Surf. Interface Anal.* **2000**, *29*, 873−886.

(21) Drysdale, N. E.; Brun, Y.; McCord, E. F.; Nederberg, F. Melt Derived Blocky Copolyesters: New Design Features for Polycondensation. *Macromolecules* **2012**, *45*, 8245−8256.

(22) Wang, Z.; Macosko, C. W.; Bates, F. S. Fluorine-Enriched Melt-Blown Fibers from Polymer Blends of Poly(butylene terephthalate) and a Fluorinated Multiblock Copolyester. *ACS Appl. Mater. Interfaces* **2016**, *8*, 754−761.

(23) Vaidya, A.; Chaudhury, M. K. Synthesis and Surface Properties of Environmentally Responsive Segmented Polyurethanes. *J. Colloid Interface Sci.* **2002**, *249*, 235−245.

(24) Synytska, A.; Appelhans, D.; Wang, Z. G.; Simon, F.; Lehmann, F.; Stamm, M.; Grundke, K. Perfluoroalkyl End-Functionalized Oligoesters: Correlation between Wettability and End-Group Segregation. *Macromolecules* **2007**, *40*, 297−305.

(25) Pilati, F.; Toselli, M.; Re, A.; Bottino, F. A.; Pollicino, A.; Recca, A. Surface Investigation by ESCA of Poly(ethylene terephthalate)-Perfluoro Polyether Block Copolymers. *Macromolecules* **1990**, *23*, 348−350.

(26) Yoon, S. C.; Ratner, B. D. Surface and Bulk Structure of Segmented Poly(ether urethanes) with Perfluoro Chain Extenders. 3. Effects of Annealing, Casting Solvent, and Casting Conditions. *Macromolecules* **1988**, *21*, 2401−2404.

(27) Baumann, E. Ueber eine einfache Methode der Darstellung von Benzoësäureäthern. *Ber. Dtsch. Chem. Ges.* **1886**, *19*, 3218−3222.

(28) Schotten, C. Ueber die Oxydation des Piperidins. *Ber. Dtsch. Chem. Ges.* **1884**, *17*, 2544−2547.

DOI: 10.1021/acs.langmuir.8b02628
Langmuir 2018, 34, 12934−12946

(29) Li, J. J. *Name Reactions: A Collection of Detailed Mechanisms and Synthetic Applications*, 5th ed.; Springer Verlag, 2014.
(30) Painter, P. C.; Coleman, M. M. *Essentials of Polymer Science and Engineering*; DEStech Publications, Inc.: Lancaster, PA, 2009; p 525.
(31) Odian, G. *Principles of Polymerization*; Wiley, 2004.
(32) Pretsch, E.; Bühlmann, P.; Badertscher, M. IR Spectroscopy. *Structure Determination of Organic Compounds: Tables of Spectral Data*; Springer: Berlin, Heidelberg, 2009; pp 1−67.
(33) Sperling, L. H. *Introduction to Physical Polymer Science*, 4th ed.; Wiley-Interscience: Hoboken, New Jersey, 2006; p 845.
(34) Fried, J. R. *Polymer Science and Technology*, 2nd ed.; Prentice Hall: Upper Saddle River, NJ, 2003; p 582.
(35) Karayannidis, G. P.; Sideridou, I. D.; Zamboulis, D. N.; Bikiaris, D. N.; Sakalis, A. J. Thermal Behavior and Tensile Properties of Poly(ethylene terephthalate-co-ethylene isophthalate). *J. Appl. Polym. Sci.* **2000**, *78*, 200−207.
(36) Luzinov, I.; Julthongpiput, D.; Tsukruk, V. V. Thermoplastic Elastomer Monolayers Grafted to a Functionalized Silicon Surface. *Macromolecules* **2000**, *33*, 7629−7638.
(37) Luzinov, I.; Xi, K.; Pagnoulle, C.; Huynh-Ba, G.; Jérôme, R. Composition Effect on the Core−Shell Morphology and Mechanical Properties of Ternary Polystyrene/Styrene−Butadiene Rubber/Polyethylene Blends. *Polymer* **1999**, *40*, 2511−2520.
(38) Wu, S. *Calculation of Interfacial Tension in Polymer Systems*; Wiley Online Library, 1971; pp 19−30.
(39) Biscerano, J. *Prediction of Polymer Properties*, 3rd ed.; Marcel Dekker, 2002.
(40) Tavana, H.; Jehnichen, D.; Grundke, K.; Hair, M. L.; Neumann, A. W. Contact angle hysteresis on fluoropolymer surfaces. *Adv. Colloid Interface Sci.* **2007**, *134−135*, 236−248.
(41) Tavana, H.; Lam, C. N. C.; Grundke, K.; Friedel, P.; Kwok, D. Y.; Hair, M. L.; Neumann, A. W. Contact angle measurements with liquids consisting of bulky molecules. *J. Colloid Interface Sci.* **2004**, *279*, 493−502.
(42) Shafrin, E. G.; Zisman, W. A. Upper Limits to the Contact Angles of Liquids on Solids. *Contact Angle, Wettability, and Adhesion*; Advances in Chemistry; American Chemical Society, 1964; Vol. *43*, pp 145−157.
(43) Sullivan, D. E. Surface Tension and Contact Angle of a Liquid−Solid Interface. *J. Chem. Phys.* **1981**, *74*, 2604−2615.
(44) Zhang, J.; Li, J.; Han, Y. Superhydrophobic PTFE Surfaces by Extension. *Macromol. Rapid Commun.* **2004**, *25*, 1105−1108.
(45) Demir, T. Synthesis and Characterization of Oleophobic Fluorinated Polyester Films. Ph.D. Thesis, Clemson University, 2015.
(46) Pilati, F.; Montecchi, M.; Fabbri, P.; Synytska, A.; Messori, M.; Toselli, M.; Grundke, K.; Pospiech, D. Design of surface properties of PET films: Effect of fluorinated block copolymers. *J. Colloid Interface Sci.* **2007**, *315*, 210−222.
(47) Cassie, A. B. D.; Baxter, S. Wettability of Porous Surfaces. *Trans. Faraday Soc.* **1944**, *40*, 546−551.
(48) Chan, C.-M. *Polymer Surface Modification and Characterization*; Hanser Publishers: Munich, 1994; p 285.
(49) Liu, Y.; Klep, V.; Zdyrko, B.; Luzinov, I. Synthesis of High-Density Grafted Polymer Layers with Thickness and Grafting Density Gradients. *Langmuir* **2005**, *21*, 11806−11813.
(50) Ton-That, C.; Shard, A. G.; Daley, R.; Bradley, R. H. Effects of Annealing on the Surface Composition and Morphology of PS/PMMA Blend. *Macromolecules* **2000**, *33*, 8453−8459.
(51) Fortin, T. J.; Laesecke, A.; Widegren, J. A. Measurement and Correlation of Densities and Dynamic Viscosities of Perfluoropolyether Oils. *Ind. Eng. Chem. Res.* **2016**, *55*, 8460−8471.
(52) Wang, Q.; Keffer, D. J.; Nicholson, D. M.; Thomas, J. B. Coarse-grained Molecular Dynamics Simulation of Polyethylene Terephthalate (PET). *Macromolecules* **2010**, *43*, 10722−10734.
(53) Cantow, M. J. R.; Larrabee, R. B.; Barrall, E. M.; Butner, R. S.; Cotts, P.; Levy, F.; Ting, T. Y. Molecular Weights and Molecular Dimensions of Perfluoropolyether Fluids. *Makromol. Chem.* **1986**, *187*, 2475−2481.
(54) Sofia, S. J.; Premnath, V.; Merrill, E. W. Poly(ethylene oxide) Grafted to Silicon Surfaces: Grafting Density and Protein Adsorption. *Macromolecules* **1998**, *31*, 5059−5070.
(55) Mei, Y.; Elliott, J. T.; Smith, J. R.; Langenbach, K. J.; Wu, T.; Xu, C.; Beers, K. L.; Amis, E. J.; Henderson, L. Gradient Substrate Assembly for Quantifying Cellular Response to Biomaterials. *J. Biomed. Mater. Res., Part A* **2006**, *79*, 974−988.
(56) Burtovyy, O. Synthesis and Characterization of Macromolecular Layers Grafted to Polymer Surfaces. Ph.D. Thesis, Clemson University, 2008.
(57) Owens, D. K.; Wendt, R. C. Estimation of the Surface Free Energy of Polymers. *J. Appl. Polym. Sci.* **1969**, *13*, 1741−1747.
(58) żenkiewicz, M. Methods for the calculation of surface free energy of solids. *J. Achiev. Mater. Manuf. Eng.* **2007**, *24*, 137−145.
(59) Rudawska, A.; Jacniacka, E. Analysis for determining surface free energy uncertainty by the Owen-Wendt method. *Int. J. Adhes. Adhes.* **2009**, *29*, 451−457.
(60) Van Krevelen, D. W. *Properties of Polymers: Their Correlation with Chemical Structure, Their Numerical Estimation and Prediction from Additive Group Contributions*, 3rd ed.; Elsevier: Amsterdam, 2000; p 875.
(61) Zenkiewicz, M. Comparative study on the surface free energy of a solid calculated by different methods. *Polym. Test.* **2007**, *26*, 14−19.
(62) Chibowski, E. Some problems of characterization of a solid surface via the surface free energy changes. *Adsorpt. Sci. Technol.* **2017**, *35*, 647−659.
(63) Chibowski, E.; Jurak, M. Comparison of contact angle hysteresis of different probe liquids on the same solid surface. *Colloid. Polym. Sci.* **2013**, *291*, 391−399.

DOI: 10.1021/acs.langmuir.8b02628
Langmuir 2018, 34, 12934−12946